Magnetic Properties of 8*H*-Type Hexagonal $Ba(Na_{1/4}Ru_{3/4})O_3$

In-Seon Kim,[#] Tetsuro Nakamura,[##] and Mitsuru Itoh*

Materials and Structures Laboratory, Tokyo Institute of Technology, 4259 Nagatsuta, Midori-ku, Yokohama 226-8503

(Received September 30, 1997)

The magnetic properties of 8*H*-type hexagonal-type $Ba(Na_{1/4}Ru_{3/4})O_3$ having a 2D geometry of $Ru^{5+}(t_{2g}{}^3)$ ions were studied by magnetic-susceptibility measurements in the temperature range 5 K $< T <$ 700 K. In this structure, the face-shared RuO_6 octahedra form $(Ru_2O_9)^{8-}$ clusters with a 2D array, which are sandwiched by 2D layers of the NaO_6 and the RuO_6 corner-shared octahedra. The magnetic data show an antiferromagnetism-like behavior, and could be well fitted to a Curie-Weiss law above 520 K with $\mu_{eff} = 3.74\ \mu_B$ and $\theta = -1330$ K. At a lower temperature range of 262 K $< T <$ 520 K, it showed a reduced magnetic moment of $\mu_{eff} = 2.32\ \mu_B$ and $\theta = -221$ K by a new Curie–Weiss law fit. The $\chi(T)$ behavior showed a strong external field dependence below 262 K, and magnetic anomaly peaks could be observed in low-field FC data at 30, 110, and 180 K, respectively. The magnetic properties of $Ba(Na_{1/4}Ru_{3/4})O_3$ are discussed concerning both a long-range 3D antiferromagnetic order and a spin-glass-like behavior.

In perovskite-type ABO_3 compounds with a relatively large *A*-site cation the tolerance factor exceeds unity; thus, an octahedral BO_6 array may be distorted compared to that in the ideal perovskite structure, and the symmetry changes to rhombohedral or hexagonal. In the hexagonal structure, the face-shared BO_6 octahedra are connected by sharing corners of the other corner-shared BO_6 octahedra in a certain stacking sequence. The face-sharing of octahedra may result from an attractive metal-metal interaction which is strong enough to overcome the repulsive metal–metal positive-core-interaction. Many hexagonal-type compounds with different stacking sequences have been reported. Hexagonal $BaTiO_3$ is a six-layer (6*H*) hexagonal with the stacking sequence *cchcch*. Other types with different stacking sequences can be stabilized in the hexagonal structure, for example, the 2*H* type of $BaNiO_3$,[1] the 3*H* type of the high-temperature form of $Ba(Zn_{1/3}Nb_{2/3})O_3$,[2] the 4*H* type of $Ba_{5/6}Sr_{1/6}RuO_3$ and $BaMnO_3$,[3,4] the 5*H* type of $Ba_5Ta_4O_{15}$,[4] the 6*H* type of $BaTiO_3$ and high-temperature form of $BaMnO_3$,[6] the 9*H* type of $BaRuO_3$,[3,4] the 10*H* type of $Ba_{10}W_6Li_4O_{30}$,[7] the 12*H* type of $Ba_4Re_2CoO_{12}$,[8,9] the 24*H* type of $Ba_4Re_2BaO_{12}$,[8,9] However, in some hexagonal compounds with the ruthenium ion in *B*-site, for example, $Ba(B'_{1/3}Ru_{2/3})O_3$ (B' = Mg, Ca, Sr, Co, Ni, Cu, Zn, and Cd)[11—14] and $Ba(B'_{1/4}Ru_{3/4})O_3$ (B' = Nb and Ta),[15] only the ruthenium ions occupy the face-shared octahedral sites. In these cases, the ruthenium ions with outer 4*d*-electrons prefer face-shared octahedral sites, and the Ru–Ru bonding is stabilized via an overlap of the half-filled or more than-half-filled t_{2g} orbitals ($t_{2g}{}^4$ and $t_{2g}{}^3$ for Ru^{4+} and Ru^{5+}, respectively) in the hexagonal structures. For $A(B'_{1/4}Ru_{3/4})O_3$ compounds, a perovskite structure stabilizes when we choose $A = Sr^{2+}$,[16] but a hexagonal structure stabilizes when $A = Ba^{2+}$.[17,18] In this case, two different kinds of hexagonal structures appear, i.e., one is the 6*H* type with a smaller B' ion of Li^+,[18] and the other is the 8*H*-type hexagonal with a bigger B' ion of Na^+, respectively. In the case of the 8*H*-type $Ba(Na_{1/4}Ru_{3/4})O_3$ with an eight-layer stacking sequence of *ccch*, the *B*-site ions, Na^+ and Ru^{5+}, settle into octahedral sites with ordered arrangements and form a quasi-two-dimensional structure. The face-shared RuO_6 octahedra form a $(Ru_2O_9)^{8-}$ cluster layer in the *c*-plane. The Ru_2O_9 cluster layers, the NaO_6 layers, and the RuO_6 layers are sequentially stacked. The magnetic susceptibility of the octahedrally coordinated Ru^{5+} ions is expected to follow a Curie–Weiss law with an effective magnetic moment of 3.78 μ_B, given by the spin-only formula, $\mu_{eff} = g\sqrt{S(S+1)}$, in the paramagnetic state at higher temperature. We could expect some various magnetic interactions of direct Ru–Ru and Ru–O–Ru superexchange couplings between the $t_{2g}{}^3$ orbitals, including a long-range 3*D* magnetic order via a diamagnetic NaO_6 octahedral layer in $Ba(Na_{1/4}Ru_{3/4})O_3$.

In this paper we describe the magnetic properties for the eight-layered (8*H*) hexagonal $Ba(Na_{1/4}Ru_{3/4})O_3$. Discussions are given on the magnetic properties of Ru^{5+} ions in $Ba(Na_{1/4}Ru_{3/4})O_3$ in terms of a pseudo-2D geometry of RuO_6 octahedra.

Experimental

1. Experimental Details. Polycrystalline samples were prepared by a solid-state reaction method with starting materials of $BaCO_3$, Na_2CO_3, and RuO_2 (all are 99.9%). A mixture of the raw materials, where 20 mol% excess of the Na_2CO_3 component over the stoichiometric composition was mixed so as to compensate for its volatilization, was pressed into pellets and fired at 1053 K for 24 h in a flow of oxygen gas. The products with excess sodium

Present address: Korea Research Institute of Standards and Science, P.O. Box 3, Taedok Sience Town, Taejon 305-606, Republic of Korea.

Present address: Department of Applied Chemistry, Utsunomiya University, 2753 Ishii-cho, Utsunomiya 321-8585, Japan.

were ground and pressed into pellets, and fired at 1173 K for 24 h in an oxygen gas flow. The pellets were ground, and washed with distilled water in order to remove any residual sodium compounds. The finally prepared pellets were fired at 1173 K for 12 h. For a Rietveld profile analysis, the powder X-ray diffraction data were recorded at room temperature by a MAC Science MPX18HF X-ray diffractometer using graphite-monochromatized Cu $K\alpha$ radiation. The magnetic susceptibilities were measured for the temperature range from 5 to 350 K by SQUID magnetometers (Quantum Design MPMS-2 at TIT and MPMS at KRISS), and for the range from 300—700 K by a Shimadzu MB-2 Faraday-type balance.

2. Experimental Result. We previously reported on the crystal structure and magnetism of a series of $Sr(B'_{1/4}Ru_{3/4})O_3$ (B' = Li and Na) compounds.[16] The result showed that these compounds stably crystallize into a perovskite structure with the space group *Pnma*. The average valence state of Ru ions in these oxides were greater than 4.9, showing that the penta-valent Ru ion was stabilized in the 6-coordinated octahedral sites. When the Ba ion is substituted for the *A*-site, the hexagonal structure is stabilized. These structures for the $Sr(B'_{1/4}Ru_{3/4})O_3$ (B' = Li and Na) and $Ba(Na_{1/4}Ru_{3/4})O_3$ are consitent with the values of their tolerance factors, i.e., t = 1.004, 0.977, and 0.947 for $Ba(Na_{1/4}Ru_{3/4})O_3$, $Sr(Na_{1/4}Ru_{3/4})O_3$, and $Sr(Na_{1/4}Ru_{3/4})O_3$, respectively. Battle et al. reported on a result concerning a neutron-diffraction experiment showing that the 8*H* hexagonal $Ba(Na_{1/4}Ru_{3/4})O_3$ has the lower-symmetry space group $P6_3mc$ (S.G. No. 186).[18] In this crystal structure, the face-shared octahedra are occupied only by Ru^{5+} ions, as in the case of $P6_3/mmc$; however, the corner-shared octahedral sites have a perfectly ordered 1 : 1 distribution of Ru and Na. By a least-squares fit of well-defined 13 Cu $K\alpha_1$ reflection lines with an internal standard of Si powder at high angles, cell parameters of a = 5.7940(2) Å and c = 19.204(1) Å could be obtained in this experiment. The octahedral arrangements in $Ba(Na_{1/4}Ru_{3/4})O_3$ are constructed on the basis of the refined atomic positional parameters,[18] and are shown in Fig. 1.

The resistivity was measured from room temperature up to 1000 K in air by a standard four-probe method. The result is shown in Fig. 2. The resistivity was very high at room temperature, and showed a semiconducting behavior with increasing temperature.

The magnetic-susceptibility data of $Ba(Na_{1/4}Ru_{3/4})O_3$ are shown in Fig. 3. The magnetic-susceptibility measurements were performed with a Faraday balance in the high-temperature range of 300 K$\leq T \leq$700 K and with SQUID magnetometers in the low-temperature range of $T \leq$ 350 K with a field cool of H = 5 kG. Our experimental results obtained with two different SQUID magnetometers (MPMS-2 at TIT and MPMS at KRISS) showed no significant difference in the measured magnetic-susceptibility data. Below room temperature, we measured the magnetic susceptibility under the field-cool condition. A magnetic field in the range from 0 G to 10 kG was applied to the sample at 300 K; then, the temperature was cooled down to 4.2 K. The magnetic susceptibility was measured with increasing temperature from 4.2 K under a magnetic field. Zero-field cool measurements were performed under magnetic fields of 10 G after zero field cool was reached. The results are shown in Fig. 4. In Fig. 5, we show the magnetic hysteresis loop of the $Ba(Na_{1/4}Ru_{3/4})O_3$ measured at 6 K and 300 K, respectively. At 6 K, the hysteresis was measured under zero field cool and field cool at 10 kG. The magnetic field was swept by ±5 kG starting from zero. The results are shown in Fig. 5(a).

Results and Discussion

The face-shared RuO_6 octahedra form $(Ru_2O_9)^{8-}$ clusters,

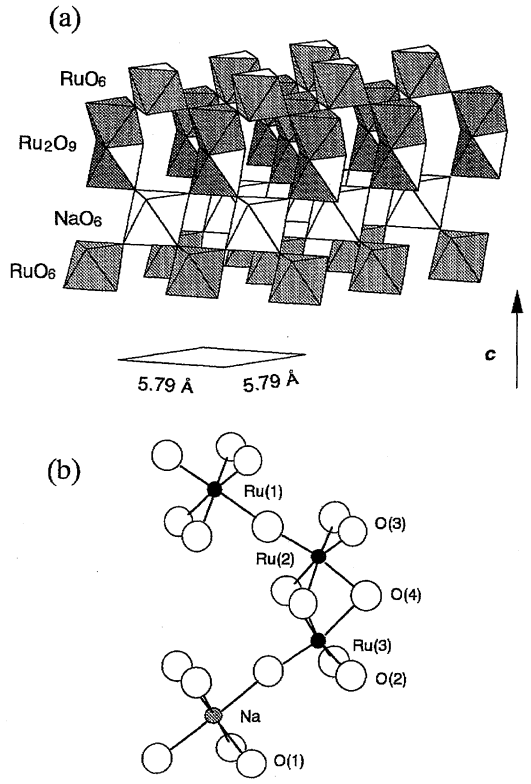

Fig. 1. Two-dimensional arrangement of RuO_6 and NaO_6 octahedra in the 8*H* structure of $Ba(Na_{1/4}Ru_{3/4})O_3$. (a); stacking of octahedra, (b); atomic coordination.

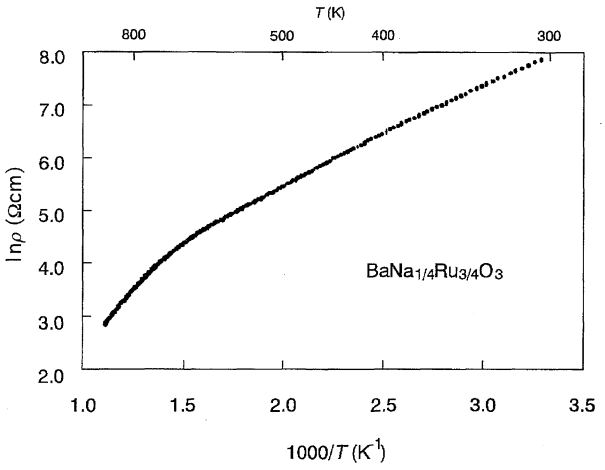

Fig. 2. Resistivity data of $Ba(Na_{1/4}Ru_{3/4})O_3$ in the temperature range 300 K < T < 1000 K.

which are arranged two-dimensionally. These Ru_2O_9 cluster layers are sandwiched by two-dimensional arrays of NaO_6 and the RuO_6 corner-shared octahedra. From Fig. 1, where Ba ions are not drawn for simplicity, two-dimensionally arranged layers of the corner-shared RuO_6 octahedra, Ru_2O_9 clusters, and NaO_6 octahedra can be well understood.

The resisvitity of $Ba(Na_{1/4}Ru_{3/4})O_3$ exhibits a semiconducting behavior with high resistivity, as shown in Fig. 2. The room-temperature resistivity was 2650 Ω cm, which is consistent with the value reported by Battle et al.[18] An activation energy of 0.17 eV could be obtained from the relation

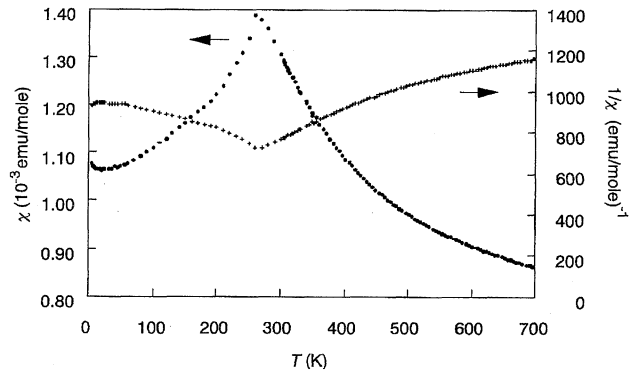

Fig. 3. Magnetic susceptibility data of $Ba(Na_{1/4}Ru_{3/4})O_3$. The magnetic susceptibility is measured with increasing temperature after field cool process ($H=5$ kG), below room temperature.

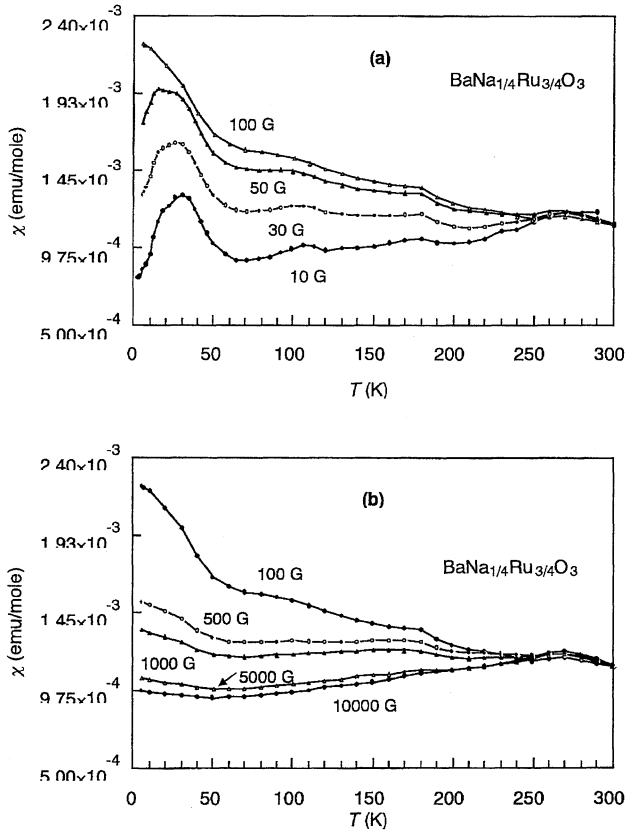

Fig. 4. Variation of the $\chi(T)$ behaviors of $Ba(Na_{1/4}Ru_{3/4})O_3$ with the various field-cool conditions.

$\sigma = \sigma_o \ln(-E_a/kT)$ in the vicinity of room temperature.

The temperature dependence of the magnetic susceptibility shows a typical antiferromagnetism-like feature with a Néel temperature of $T_o \approx 262$ K, if one sees the FC ($H=5$ kG) data, as shown in Fig. 3. However, the inverse of the magnetic-susceptibility data shows three different $\chi(T)$ behaviors quite clearly. Above 520 K in the spin non-correlated paramagnetic region, the magnetic susceptibility data obey the Curie–Weiss law, with $\theta = -1332$ K. The calculated effective magnetic moment from the Curie constant is $\mu_{eff} = 3.74\ \mu_B$. The effective magnetic moment in the paramagnetic phase

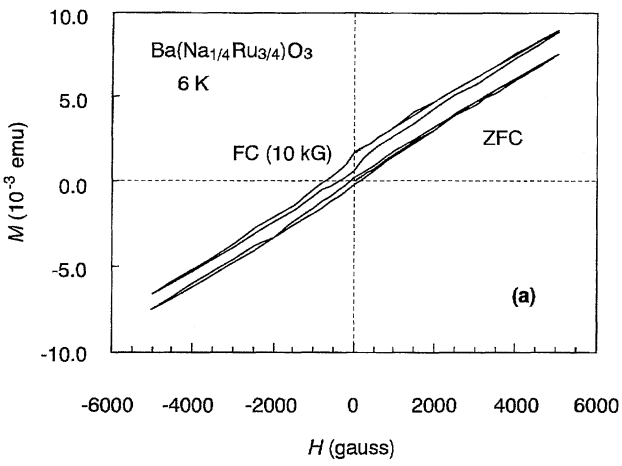

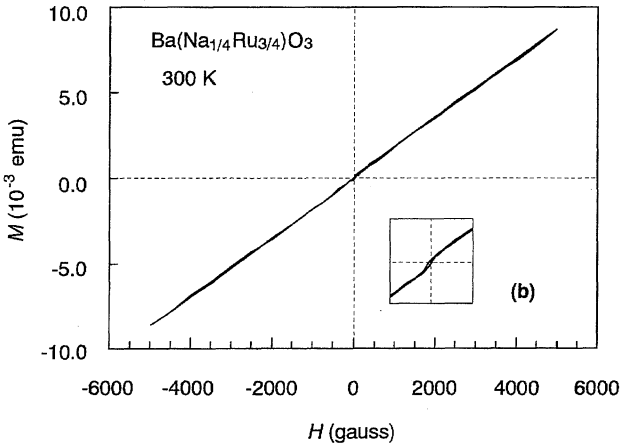

Fig. 5. Magnetic hysteresis loop of $Ba(Na_{1/4}Ru_{3/4})O_3$ measured at 6 K (a), and at 300 K (b).

of $Ba(Na_{1/4}Ru_{3/4})O_3$ is consistent with the value of the spin-only value ($g\sqrt{S(S+1)}$) of the t_{2g}^3 configuration of the Ru^{5+} ion. In the temperature range $262\ K < T < 520$ K, the slope in $1/\chi(T)$ changes from that of the higher temperature region. The constants $\theta = -221$ and $\mu_{eff} = 2.32\ \mu_B$ could be obtained from a new Curie–Weiss law fit.

The quite reduced effective magnetic moment of $Ba(Na_{1/4}Ru_{3/4})O_3$ in the range $262\ K < T < 520$ K indicates that some spin-correlations among the Ru^{5+} ions do exist. We would expect several kinds of magnetic interactions in $Ba(Na_{1/4}Ru_{3/4})O_3$, the Ru–Ru direct intracluster interaction, the Ru–O(2)–Ru superexchange interaction, the interlayer interaction between Ru_2O_9 cluster and the corner shared-octahedra, and the Ru(1)–O–Na–Ru(3) long-range interlayer interactions via a 2-D array of NaO_6 octahedra. Among them, the direct Ru–Ru interaction is considerably strong, and dominantly determines the magnetic properties, because the Ru–Ru separation is relatively small and the t_{2g} orbital stabilized by the resulting trigonal field is directed towards the common face.[23] The low value of the effective magnetic moment observed in the spin-correlated paramagnetic range (262—520 K) is considered to be associated with the magnetic spin interaction in the Ru_2O_9 cluster among mostly

antiferromagnetic, but imperfectly antiferromagnetically ordered, Ru^{5+} ions.

The magnetic susceptibility of $Ba(Na_{1/4}Ru_{3/4})O_3$ becomes divergent along with a variation of the external cooling field at $T \leq 262$ K, as can be seen in Fig. 4. The $\chi(T)$ at low temperature shows a very complex behavior in the low-field FC data. As shown in Fig. 4(a), four magnetic anomalies can be observed at 262, 180, 110, and 30 K. The peak positions of the first three anomalies are consistent with the result of Battle et al., while their $\chi(T)$ data show quite different behaviors compared to our data below 262 K. The last three peaks in this report disappear when the external field (H) is increased, i. e., the 30 K peak disappears when $H > 50$ G, the 110 K peak when $H > 100$ G, and the 180 K peak when $H > 5$ kG, respectively, while the 262 K peak is not influenced at all. Below 262 K, the nearest-neighbor superexchange interactions, being of comparable strength, stabilize an antiferromagnetic ordering of Ru^{5+} ions in the face-shared and the corner-shared RuO_6 octahedra. The peak at 180 K may be associated with the pseudo-2D weak ferromagnetic correlations of Ru^{5+} ions in the corner-shared RuO_6 octahedra. A spin reorientation occurs at 110 K. The peak at ca. 30 K in ZFC is considered to be associated with the onset of a dynamic crossover, which may be related to a long-range 3D antiferromagnetic order involving the NaO_6 octahedra; it is observed only when a low external field is applied. As shown in Fig. 4(a), the 30 K magnetic anomaly peak shows a tendency of decreasing the peak temperature as H is increased. The peak position was measured to be 30, 23, and 18 K at $H = 10$ G, $H = 30$ G, and $H = 50$ G, respectively. At $H = 100$ G, the anomaly peak is not observable down to 5 K (the lower limit of our experiments), but looks like a peak exists at around 5 K, or just below. As the cooling field was increased above 100 G, the anomaly apparently disappeared, accompanying a decrease of χ with increasing H at lower temperature, as can be seen in Fig. 5(b). This type of magnetic anomaly peak behavior at a low field has been observed in Na_3RuO_4. The rock-salt related compound of Na_3RuO_4, in which Ru_4O_{16} clusters are isolated by NaO_6 octahedra, exhibits a long-range 3D antiferromagnetic ordering with a Neel temperature of 30 K.[25]

In Fig. 5, we show the results of magnetic hysteresis-loop measurements of $Ba(Na_{1/4}Ru_{3/4})O_3$. A displacement of the hysteresis loop is observed in the FC data, which were measured at 6 K with a 10 kG field cool process, as shown in Fig. 5(a).

The $\chi(T)$ behaviors of $Ba(Na_{1/4}Ru_{3/4})O_3$ discussed so far, e.g., the divergence of χ below the cusp at 262 K, the displacement of the hysteresis loop and the variation in the peak position at 30 K, suggest further examples of spin-glass-like behaviors. A reduce effective magnetic moment is observed in the spin-glasses of Sr_2FeNbO_6[21] and in $FeSbO_4$.[22] The Sr_2FeNbO_6 perovskite is reported to show three different magnetic behaviors along with a variation of the temperature. It shows an effective magnetic moment of $\mu_{eff} = 5.8$ μ_B in the temperature range $T > 700$ K, and follows a new Curie–Weiss law with $\mu_{eff} = 3.4$ μ_B in the temperature range 32.5 K $< T <$ 700 K. It shows a spin-glass state below 32.5 K. The rutile-related dilute antiferromagnetic $FeSbO_4$ shows an effective magnetic moment of $\mu_{eff} = 6.0$ μ_B and $\mu_{eff} = 3.2$ μ_B in the temperature ranges 300 K $< T <$ 1000 K and 70 K $< T <$ 300 K, respectively. The magnetic susceptibility exhibits a divergence between ZFC and FC below ca. 70 K, entering a spin-glass state. The disappearance of magnetic anomaly peaks with increasing magnetic field has been observed in spin-glasses of $Eu_{0.1}Sr_{0.9}S$[24] and $FeSbO_4$. A variation in the position of the $\chi(T)$ peaks was observed in the spinel spin-glass of Co_2TiO_4, and was explained according to the Gabay and Toulouse theory (Ref. 26 and references therein). Gabay and Toulouse have shown that it is possible to have three phase transitions: paramagnetic state $\overset{T_C,T_N}{\longleftrightarrow}$ ferro/ferri/antiferromagnetic state $\overset{T_{M1}}{\longleftrightarrow}$ mixed phase 1 $\overset{T_{M2}}{\longleftrightarrow}$ mixed phase 2. More than three susceptibility peaks can occur in any system if the x and y components of the spin do not freeze simultaneously at T_{M1}, but freeze at two different temperatures, say T'_{M1} and T''_{M1}.

The most prominent features of the spin-glass behavior are a cusp in the temperature dependence of the susceptibility at the freeze temperature, a divergence of the susceptibility below the temperature depending on the field cool history, and a displacement of the hysteresis loop in the field cool process below the freezing temperature.[27] The bond frustration has been identified as being due to a spin-glass behavior. The frustration may be due to competition between interactions of different signs, or it may be inherent in the underlying lattice in a system with antiferromagnetic interactions. In the spin-glasses, the magnetic interactions are predominantly short range. The lack of magnetic Bragg reflections at low temperature suggests that $Ba(Na_{1/4}Ru_{3/4})O_3$ is a strong frustrated magnetic system.[28] A cationic order may result in the next-nearest-neighbor super-exchange interactions being of comparable strength to the nearest-neighbor interactions, and may thereby destabilize the long-range antiferromagnetic ordering, but with a magnetic frustration which is insufficient to produce a true spin-glass phase transition where the magnetic correlation is of much shorter range. Finally, we must refer to the randomness of the system. As the result of the mentioned structural analysis, $Ba(Na_{1/4}Ru_{3/4})O_3$ has a completely ordered B-site arrangement. Thus, the strength of the competitive magnetic interactions depend on the temperature. Recently, our group has succeeded in controlling the order parameter of B-site ordered perovskites, $Sr(Fe_{1/2}Bi_{1/2})O_3$ and $Ba(Fe_{1/2}Bi_{1/2})O_3$. Both these compounds were found to exhibit a spin-glass behavior.[29] The effect of the randomness and bond frustration on the spin glass behavior will be discussed in detail in the next paper.

All of the usual features of a spin-glass are observed in the $\chi(T)$ behaviors of $Ba(Na_{1/4}Ru_{3/4})O_3$, and the magnetic anomaly peaks at 262, 180, 110, and 30 K are considered to correspond to the phase-transition temperatures of T_N, T_{M1}, and T_{M2} in a spin-glass, as predicted by Gabay and Toulouse.

Conclusions

In the eight-layer hexagonal $Ba(Na_{1/4}Ru_{3/4})O_3$ having ordered *B*-site cations of Na and Ru ions, the corner-shared RuO_6 octahedra and NaO_6 octahedra, as well as the Ru_2O_9 clusters are arranged in a layered structure having 2D geometry, respectively. Ru^{5+} ions in the compound have half-filled t_{2g} orbitals. In the face-shared octahedra of Ru_2O_9 clusters, the t_{2g} orbitals directed toward the common face and the Ru–Ru metal bonding is stabilized. From the view point of crystal structure, very complex magnetic interactions are expected, such as direct interactions, and superexchange interactions, as well as interlayer long-range interactions.

The magnetic-susceptibility data of $Ba(Na_{1/4}Ru_{3/4})O_3$ over a wide temperature range (10— 700 K) with FC data below room temperature showed an antiferromagnetism-like feature, and could be fitted to a Curie–Weiss law at high temperature (>520 K), resulting in $\theta = -1332$ K and an effective magnetic moment of 3.74 μ_B, which is consistent with the spin-only formula for a localized d^3 ion without any orbital contribution. In the temperature range 262 K < T < 520 K, it showed a reduced effective magnetic moment of $\mu_{eff} = 2.32$ μ_B, and $\theta = -221$ K by a new Curie–Weiss law fit. The low-field FC data of $\chi(T)$ showed four magnetic anomalies at 30, 110, 180, and 262 K, respectively. The 30 K peak in $\chi(T)$ is considered to be a long-range 3D antiferromagnetic order involving a NaO_6 octahedra layer. The magnetic susceptibility of $Ba(Na_{1/4}Ru_{3/4})O_3$ showed a strong field dependence below 262 K in $\chi(T)$, and a displacement of the hysteresis loop in the FC process. Not only these features, but a quite reduced effective magnetic moment at lower temperature in the paramagnetic-state region, strongly suggest evidence of a spin-glass state transition in $Ba(Na_{1/4}Ru_{3/4})O_3$. To prove a real spin-glass transition of $Ba(Na_{1/4}Ru_{3/4})O_3$, much more intense studies are needed.

Part of this work was carried out unber a Grant-in-Aid for Scientific Research from Ministry of Education, Science and Culture and JSPS Research for Future Program, "ATOMIC-SCALE SURFACE AND INTERFACE DYNAMICS".

References

1) R. A. Gardner, *Acta Crystallogr., Sect. B*, **B25**, 781 (1969).
2) U. Treiber and S. Kemmler-Sack, *J. Solid State Chem.*, **43**, 51 (1982).
3) P. C. Donohue, L. Katz, and R. Ward, *Inorg. Chem.*, **4**, 306 (1965); P. C. Donohue, L. Katz, and R. Ward, *Inorg. Chem.*, **5**, 339 (1966).
4) J. B. Goodenough and J. M. Longo, "Landolt-Bornstein," Springer-Verlag, New York (1970), New Series, Group III/Vol. 4a.
5) F. Galasso and L. Katz, *Acta Crystallogr.*, **14**, 647 (1961).
6) A. Hardy, *Acta Crystallogr.*, **15**, 179 (1962).
7) T. Negas, R. S. Roth, H. S. Parker, and W. S. Bower, *J. Solid State Chem.*, **8**, 1 (1973).
8) L. Katz and R. Ward, *Inorg. Chem.*, **3**, 205 (1964).
9) O. Muller and R. Roy, "The Major Ternary Structural Families," Springer-Verlag, Berlin (1974).
10) B. M. Collins, A. J. Javobson, and B. E. F. Fendor, *J. Solid State Chem.*, **10**, 29 (1974).
11) A. Callaghan, C. Moeller, and R. Ward, *Inorg. Chem.*, **5**, 1572 (1966).
12) J. Darriet, M. Drillon, G. Villeneuve, and P. Hagenmuller, *J. Solid State Chem.*, **19**, 213 (1976).
13) R. C. Byrne and C. W. Moeller, *J. Solid State Chem.*, **2**, 228 (1970).
14) I. Fernandez, R. Greatrex, and N. N. Greenwood, *J. Solid State Chem.*, **34**, 121 (1980).
15) R. Greatrex and N. Greenwood, *J. Solid State Chem.*, **31**, 281 (1980).
16) I. S. Kim, T. Nakamura, M. Itoh, and Y. Inaguma, *Mat. Res. Bull.*, **28**, 1029 (1993).
17) I. S. Kim, T. Nakamura, M. Itoh, and Y. Inaguma, "Proceedings of 9th Korea–Japan New Ceramics Seminar," (1992), Abstr., p. 393.
18) P. D. Battle, S. H. Kim, and A. V. Powell, *J. Solid State Chem.*, **101**, 161 (1992).
19) F. Izumi, "The Rietveld Method," Oxford University Press, Oxford (1992), Chap. 13.
20) R. D. Shannon, *Acta Crystallogr., Sect. A*, **A32**, 751 (1976).
21) R. Rodriguez, A. Fernandez, A. Isalgue, J. Rodriguez, A. Labarta, J. Tejada, and X. Obradors, *J. Phys. C: Solid State Phys.*, **18**, L401 (1985).
22) X. Obradors, J. Bassas, J. Rodriguez, J. Pannetier, A. Labarta, J. Tejada, and F. J. Berry, *J. Phys.: Condens. Matter.*, **2**, 6801 (1990).
23) J. B. Goodenough, "Magnetism and the Chemical Bond," John Wiley & Sons, New York– London (1963).
24) H. Maletta and W. Felsch, *Phys. Rev. B*, **B20**, 1245 (1979).
25) T. C. Gibb, R. Greatrex, and N. N. Greenwood, *J. Solid State Chem.*, **31**, 153 (1980).
26) J. K. Srivastava, J. A. Kulkarni, S. Ramakrishnan, S. Singh, V. R. Marathe, G. Chandra, V. S. Darshane, and R. Vijayaraghavan, *J. Phys. C: Solid State Phys.*, **20**, 2139 (1987).
27) P. M. Levy, C. Morgan-Pond, and A. Fert, *J. Appl. Phys.*, **53**, 2168 (1982).
28) S. H. Kim, private communications.
29) M. Itoh, unpublished work.